

**Core-level photoemission study of the InAs/CdSe nanocrystalline system**

C. McGinley\*

*HASYLAB/DESY, Notkestrasse 85, D-22607 Hamburg, Germany*

H. Borchert and D. V. Talapin

*Institut für Physikalische Chemie, Universität Hamburg, D-20146 Hamburg, Germany*

S. Adam and A. Lobo

*HASYLAB/DESY, Notkestrasse 85, D-22607 Hamburg, Germany*

A. R. B. de Castro

*Laboratorio Nacional de Luz Sincrotron, Campinas 13081-90, Brazil*

M. Haase and H. Weller

*Institut für Physikalische Chemie, Universität Hamburg, D-20146 Hamburg, Germany*

T. Möller

*HASYLAB/DESY, Notkestrasse 85, D-22607 Hamburg, Germany*

(Received 14 July 2003; published 6 January 2004)

We have applied the technique of core-level photoemission spectroscopy with synchrotron radiation to a study of the interface in the colloiddally prepared InAs/CdSe core/shell nanocrystal system. We find that As-Se and In-Se chemical bonds dominate the interface which we may describe as “Se rich.” The surface states observed for In and As of the pure InAs nanocrystals are successfully removed by growth of the CdSe shell layer. We discuss how the removal of these “surface charge traps” causes a large increase in the photoluminescence yield compared with that of the pure InAs nanocrystal.

DOI: 10.1103/PhysRevB.69.045301

PACS number(s): 79.60.Bm, 61.46.+w, 73.20.-r

**I. INTRODUCTION**

In the area of nanotechnology semiconductor nanocrystals are known as one of the most important advanced materials. The most remarkable features of these nanocrystals are their specific chemical and physical properties, among which the high photoluminescence is of great interest. Often the pure nanocrystals have a low luminescence yield due to insufficient passivation by organic ligands. The defects at the nanocrystal surface give rise to nonradiative recombination processes resulting in poor luminescence quantum yield. The growth of a thin epitaxial layer (shell) surrounding the pure nanocrystal (core) reduces the defect concentration, forming a highly ordered interface and thereby suppressing the nonradiative recombination processes.<sup>1-3</sup>

Hence the core/shell nanocrystals combine the qualities of the quantum dot size-dependent band gap<sup>1</sup> with the high-fluorescence yield arising from a well passivated surface.<sup>2</sup> Using III-V nanocrystals with a narrow particle size distribution for the core with an epitaxially grown shell of a larger band gap II-VI material produces systems with ideal “artificial atom” electronic states,<sup>3</sup> which are highly stable against oxidation as compared with the cores and also show very high photostability in comparison with laser dyes.<sup>4</sup> CdSe/CdS,<sup>5</sup> CdSe/ZnS,<sup>6</sup> CdS:Mn/ZnS (Ref. 7) are some examples for core/shell structures of different semiconductor materials.

While II-VI semiconductor nanocrystals were studied extensively during the last two decades, much less information

is available about their III-V analog. On the other hand, III-V nanocrystals can exhibit even more pronounced quantum size effects than II-VI materials, as they have relatively covalent bonding and direct band-gap structure, larger bulk exciton radii, and smaller effective masses of electron and holes. The band gap of bulk InAs is 0.46 eV at room temperature corresponding to the absorption onset at 2.7  $\mu\text{m}$  so that the excitonic transitions of InAs nanocrystals appear in the near-IR spectral region. The luminescent properties of as-prepared InAs nanocrystals are rather poor (the room-temperature photoluminescence quantum efficiency is about 1%).<sup>8</sup> Fortunately, the growing around InAs nanocrystals an epitaxial shell of a wider band gap II-VI semiconductor (e.g., CdSe or ZnSe) allows increasing their luminescent efficiency up to 15–18%.<sup>4</sup> These InAs based core-shell nanocrystals attract great interest because of their potential applications in light-emitting devices for the near-infrared (NIR) spectral range used in telecommunications<sup>9</sup> and luminescent biological labels.<sup>10</sup>

We have studied the internal core/shell interface of InAs/CdSe by photoelectron spectroscopy with synchrotron radiation and compare results found from the pure cores of InAs in order to find the local origin of the improved optical properties in the core/shell nanocrystal. We have recorded core level spectra from the four atom types present with differing photon energies so that the contrast in kinetic energy ranges gives a variation of the surface sensitivity in the measurements. This allows us to distinguish between atoms in the volume of the core and those at the interface. Resulting core

level shifts indicate the amount of charge transfer or surface strain involved at the interface.

## II. EXPERIMENT

InAs/CdSe core-shell nanocrystals were synthesized via two-stage colloidal chemical synthesis described in Ref. 4. Nearly monodisperse InAs nanocrystals were prepared and further coated with the epitaxial shell of CdSe. The surface of both InAs and core-shell nanocrystals was capped with a shell of tri-*n*-octylphosphine (TOP) molecules which passivate surface dangling bonds and provide to the nanocrystals solubility in a variety of nonpolar solvents such as toluene, hexane, and chloroform. The optical measurements were performed by dissolving the nanocrystals in toluene and recording absorption and photoluminescence (PL) spectra. UV-NIR absorption spectra were taken on a Cary 500 (Varian) spectrophotometer. PL spectra in the near-IR spectral region were measured with a Fluorolog-3 (Instruments SA) spectrofluorimeter. All PL spectra of colloidal solutions were measured at optical densities at the excitation wavelength (600 nm) below 0.1. To compare the PL efficiencies of different samples, we normalized each PL spectrum with respect to the absorbed light intensity at the excitation wavelength and subsequently integrated the PL intensity versus photon energy over the entire emission spectrum.

Colloidal solutions of nanocrystals were deposited onto Au substrates and the solvent allowed to evaporate in an N<sub>2</sub> atmosphere. Samples were transported in sealed N<sub>2</sub> flasks to the experimental chamber into which they were transferred using a fast-entry load lock. The quality of the core level and valence band spectra showed that no excessive oxidation of the samples took place during their ~1 min exposure to the ambient atmosphere. A chamber base pressure of  $5 \times 10^{-10}$  mbar was maintained during photoemission experiments. Spectra were recorded using an Omicron EA125 hemispherical electron spectrometer (HEA) and the SX700 beamline monochromator provided photons in the 90–650 eV energy range for this work. A combined experimental resolution (photon source and HEA) of 200 meV was selected here for spectra recorded at photon energies below 200 eV. At higher photon energies the resolution decreases to ~300 meV, but higher resolution was not necessary as the width of the core level spectra are dominated by material effects such as inhomogeneous Fermi level pinning caused by surface and interfacial defects. A high count rate was thus achieved with the undulator radiation, no radiation damage was observed over time and charging effects were not observed. Our finding that charging effects are not present is in contrast to measurements on thiol terminated II-VI nanocrystals where sample charging via a surface photovoltage had a large effect on the photoemission spectra.<sup>11</sup>

## III. RESULTS AND DISCUSSION

Absorption and photoluminescence spectra of the InAs and InAs/CdSe nanocrystals are shown in Fig. 1. The well-resolved first excitonic transition at 1.34 eV observed in the absorption spectrum of InAs nanocrystals indicates a narrow

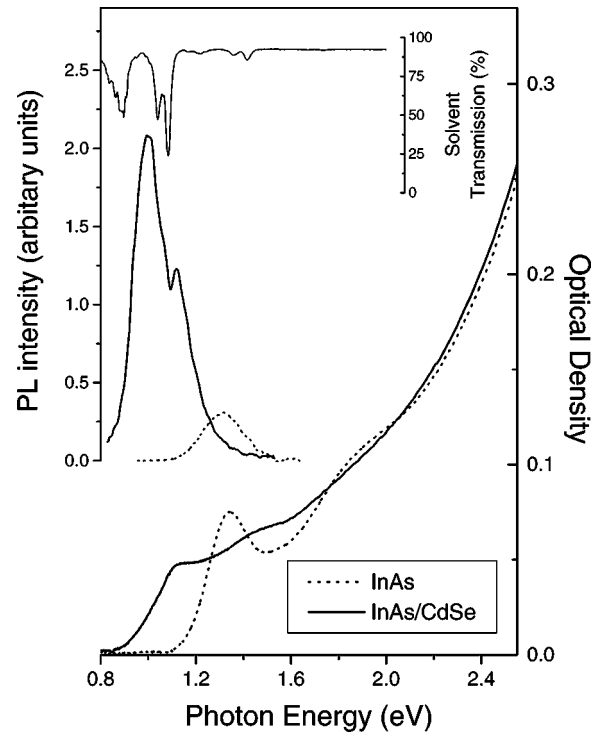


FIG. 1. Absorption (optical density) and photoluminescence spectra for the TOP capped InAs and InAs/CdSe nanocrystals dissolved in toluene. An absorption spectra of neat toluene is also shown.

particle size distribution. The size of InAs nanocrystals used as cores for growing InAs/CdSe core-shell particles was estimated as  $29 \pm 3$  Å by high-resolution transmission electron microscopy measurements. Growth of CdSe shell around InAs nanocrystals results in redshift of both absorption and PL spectra because the electron wave function extends to the CdSe shell, and its confinement energy is lowered.<sup>4</sup> Also, the CdSe shell provides effective passivation of InAs surface states (nonradiative recombination channels) and the shell growth accompanies with significant increase of PL efficiency by approximately one order of magnitude. Exact estimation of the PL quantum efficiency of InAs/CdSe core-shell nanocrystals is difficult because the emission spectrum of core-shell nanocrystal partially overlaps with an absorption band of toluene used as a solvent (Fig. 1). As a result, a significant portion of emitted light is absorbed by toluene.

To describe the InAs/CdSe interface we now discuss the fitted core level spectra for the system. Core level spectra were recorded for a range of photon energies and subsequently fitted to the minimum number of Voigt functions using a simplex optimization routine. The relevant fitting parameters are shown in Table I and are in agreement with those found by earlier authors for In 4*d* (Refs. 12 and 13) and As 3*d* (Refs. 14 and 15). Figures 2(a) and 2(b) show spectra of the Cd 3*d*<sub>5/2</sub> and Se 3*d* core levels at surface sensitive energies where we see that the data are well fitted using one Voigt function only. In contrast, spectra of the As 3*d* core level in Fig. 3(a) show a surface, or in this system an interfacial, core level shift (ICLS) which is made clear by com-

TABLE I. Core level spectra fitting parameters (all quantities are in eV).  $\Gamma$  is the Gaussian broadening of a particular Voigt component.

	In $3d_{5/2}$	In $4d^a$	In $4d^b$	As $3d^a$	As $3d^b$	Cd $3d_{5/2}$	Se $3d$
$\Gamma_V$	0.80	0.67	0.62	0.65	0.57	0.99	0.88
Lorentzian	0.40	0.155	0.155	0.17	0.17	0.27	0.19
S.O. split.		0.85	0.85	0.69	0.69		0.88
ICLS ( $I$ )	-0.88(05)	-0.72		-0.70(05)			
$\Gamma_I$	0.80	2.08		1.63			
SCLS ( $S_1$ )			-0.44(05)		-0.22(05)		
$\Gamma_{S_1}$			1.80		1.26		
SCLS ( $S_2$ )			-2.4(0.1)		-1.40(30)		
$\Gamma_{S_2}$			1.60		1.11		

<sup>a</sup>InAs/CdSe-TOP nanocrystals.

<sup>b</sup>InAs-TOP nanocrystals.

paring fitted spectra recorded using a range of photon energies. In Fig.3(b) we show an As  $3d$  spectra<sup>16</sup> recorded in identical conditions for InAs nanocrystals coated with TOP for comparison with the InAs/CdSe data above. Both spectra are fitted, as usual, with the minimum number of Voigt components and it is not possible to achieve the same number of these for both curves, even allowing the maximum number of variable fitting parameters. The two components of the InAs-TOP system cannot be replaced by one broad component similar to the InAs/CdSe data. Our earlier assignment of

the surface core-level shifts (SCLS) in pure InAs nanocrystals as being due to purely surface As and As atoms bonded to P atoms of the TOP ligands is therefore justified. From the As  $3d$  data of the InAs/CdSe system we see that no As-P bonds exist and the rehybridized surface As atoms, found in many III-V clean surface studies, are absent. The new component ( $I$ ) in Fig. 3(a) here has a shift in kinetic energy relative to the primary volume peak of  $-0.70 \pm 0.05$  eV. This compares quite well with the  $-0.80$  eV found for the As  $3d$  SCLS due to As-Se bonds in the ZnSe-GaAs(001) hybrid interface system.<sup>17</sup> In general, an As  $3d$  SCLS of 1 eV is typical for an As-Se surface chemical bond in Se treated GaAs surfaces.<sup>18</sup> We observe no distinct surface state due to As atoms with lowered coordination number in InAs/CdSe a point which we return to below in discussing how the growth of a shell layer removes the surface charge traps found in the InAs system.

As the surface chemical bonding for As atoms is quite different for the core/shell and core-only systems we show in Fig. 4 the In  $3d_{5/2}$  core level spectra for InAs/CdSe. Two components due to photoemission from volume and interfacial In atoms are observed, the ICLS is  $-0.88 \pm 0.05$  eV in kinetic energy.

In  $4d$  core level spectra were also recorded but those in the low-kinetic-energy range overlap in a complex manner with the Cd  $4d$  level due to the valence-band-induced dispersion of the latter. The size of the ICLS is, however, the similar for both In  $3d$  and  $4d$  core levels and we associate this component with emission from interfacial In atoms bonded to Se as was the case for As atoms above. Again the magnitude and direction of the ICLS are consistent with the relative electronegativities of In and Se.

We see no evidence here for Cd-As interfacial bonding in either the Cd  $3d$  or As  $3d$  core level which could possibly give rise to a high-kinetic-energy side ICLS in the As  $3d$  spectra. May be this kind of As  $3d$  ICLS would not be distinguishable in this experiment, but we know that a Cd rich surface would suppress those ICLS's in both Se  $3d$  and As  $3d$  which we do see here (see Ref. 17 for photoemission from a group II rich interface). Our evidences for In-Se and As-Se interfacial bonds only are somewhat similar to our

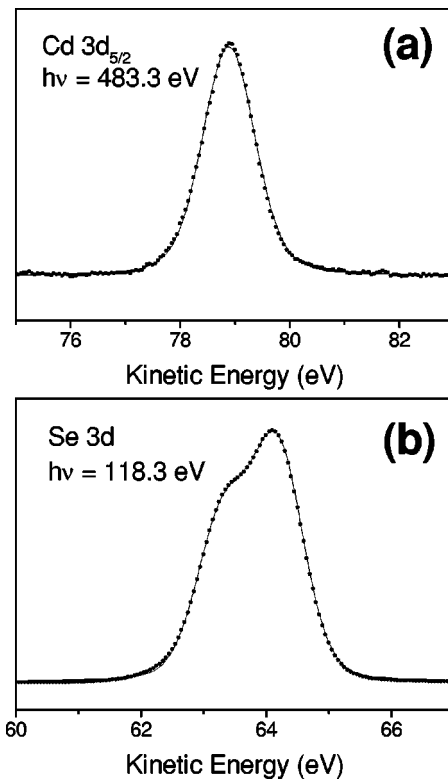


FIG. 2. Photoelectron spectra of the Cd  $3d_{5/2}$  and Se  $3d$  core levels recorded at surface sensitive photon energies. The data are represented by dots with the fitted Voigt function as a full line. No surface or interfacial core level shifts exist.

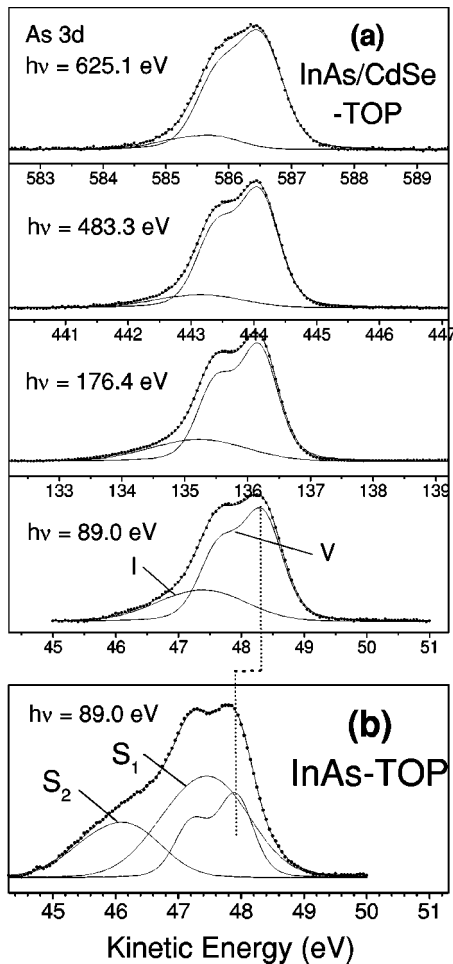


FIG. 3. As  $3d$  core level photoelectron spectra recorded over a range of photon energies for InAs/CdSe (a). This emphasizes the significance of the interfacial component ( $I$ ) compared to the volume component ( $V$ ) at low, surface sensitive photon energies. (b) shows As  $3d$  data for the pure InAs quantum dot which with comparison to the core/shell data justifies the assignment of components  $S_1$  and  $S_2$  with surface As and As-P bonds.

conclusions for the InAs-TOP systems.<sup>16</sup> In this pure quantum dot we saw In-P and As-P bonds formed, i.e., both anions and cations bond to the group V atoms of the organic ligands. Here, for the core/shell, In and As are bonded to the group VI atom Se only implying that the interface is Se rich. Our results therefore are again similar, especially for the group III In  $3d$  core level spectra, to photoemission results for the GaAs/ZnSe molecular beam epitaxy grown interface where a Ga-Se chemical bond gave rise to a Ga  $3d$  core level shift of  $-0.6$  to  $-0.8$  eV.<sup>17</sup>

Returning to the spectra for the shell atoms where we observe no core level shift for Cd  $3d$  and Se  $3d$ , no shifts were found for the II-VI layer in the GaAs/ZnSe system despite the fact that up to  $40$  Å of ZnSe were grown with a surface reconstruction evident from reflection high-energy electron diffraction patterns.<sup>17</sup> Lowered surface symmetry which is well ordered enough to be visible via electron diffraction is normally expected to produce core level shifts.

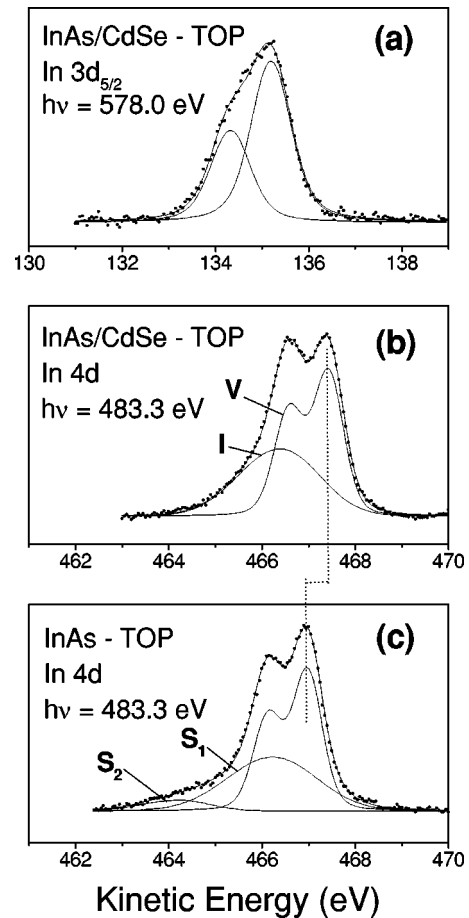


FIG. 4. Photoelectron spectra for InAs/CdSe of (a) the In  $3d_{5/2}$  and (b) the In  $4d$  core levels which show an In interfacial component ( $I$ ) and in (c) the In  $4d$  core level of InAs-TOP. Comparison of spectra (b) and (c) shows that components  $S_1$  and  $S_2$  are removed by the growth of CdSe and were previously correctly identified with surface In and In bonded to P.

That ZnSe core level spectra show no such shifts in a heterojunction is similar to what we see here: we see shifts neither due to the interface nor due to Cd or Se bonding to P of the ligand molecules. Such bonds show very large shifts in the case of InAs-TOP [see Fig. 3(b)]. We may, however, be sure of the state of the InAs surface in InAs/CdSe and discuss reasons as to how the photoluminescence yield of the InAs is dramatically increased by the surface changes which occur with the growth of the CdSe shell.

Early work on fluorescence limitation suggested that in II-VI particles hole traps at the surface were the cause of dark channel exciton recombination.<sup>1</sup> A more recent theoretical calculation for InP quantum dots<sup>19</sup> showed that unpassivated surface anions (group V) and cations (group III) have dangling bond states which act as hole and electron traps, respectively. Components  $S_1$  in the As  $3d$  and In  $4d$  core level spectra from InAs-TOP [Figs. 3(b) and 4(c)] are compatible with these types of surface states although here they are slightly oxidized.<sup>16</sup> The dangling bonds have the form of a filled  $s^2p^3$  As orbital and an empty  $sp^2$  In orbital. With the growth of the CdSe shell both of these surface states are

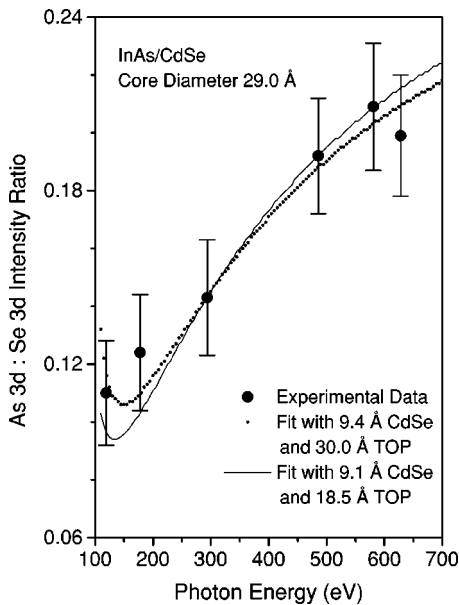


FIG. 5. As 3d:Se 3d core level intensity ratio as a function of photon energy. Fitting of the data yields the dimensions of the outer layers of the core/shell nanocrystal.

removed and replaced by As-Se and In-Se bonds, respectively. This is, we believe, the origin of the order of magnitude increase in the photoluminescence of these particles.

We also compared intensity ratios of core level spectra recorded at different photon energies and therefore differing kinetic-energy ranges. The surface sensitivity varies with electron kinetic energy so by plotting the intensity ratio of the As 3d to Se 3d core level signals as a function of the photon energy we show that Se (As) lies predominantly in the shell (core) of the system. This is shown in Fig. 5 along with a simulation of the intensity ratio versus photon energy curve. A full description of this simulation method is published elsewhere<sup>20</sup> and is a variation on a method used to find dopant atom distributions in *n*-type nanoparticles.<sup>21</sup> Briefly, we recorded photoelectron spectra of the As and Se 3d core levels at a series of different photon energies. The Se:As photoemission ratio was normalized for the detector sensitivity function, photoionization cross section, and the asymmetry term.<sup>20,21</sup> The simulated curve takes into account the electron mean-free path in all three material types for each kinetic energy and the simulation was for a spherical sample where the InAs core diameter was known precisely (29.0 Å). The best data fit yields the thickness of the CdSe shell, a measurement which is normally difficult to make by TEM, for example, where the interface between the two types of material is not at all obvious.

The data simulation curves in Fig. 5 represent limiting values and fit the data well. The best fit is obtained with 9.4 Å for the CdSe shell thickness and 30 Å for the TOP shell thickness. The hooklike shape of the simulated curve at low photon energies is due to the dependence of photoelectron mean-free path on the kinetic energy, which was calculated using TPP-2M formula of Tanuma, Powell, and Penn.<sup>22,23</sup> TPP-2M formula gives a better precision in calculating elec-

tron mean-free path at higher kinetic energies, however, in the range of 50–200 eV the formula does not represent accurately the different inelastic scattering phenomena and hence, in Fig. 5, we find at low photon energies, where the kinetic energies of As 3d and Se 3d are below 200 eV, the data points are slightly deviated from the simulated curves. A second simulation curve is plotted with parameters of 9.1 Å and 18.5 Å. This curve still results in a reasonable representation of the experimental data and reveals a fundamental difference in the precision of the method for determining the layer thicknesses of the CdSe and the ligand shell, respectively. The routine is more reliable for estimating the thickness of the CdSe shell than that of the ligand shell. While all reasonable simulation curves lead to values around 9.0–9.5 Å for the CdSe shell, the uncertainty in the ligand shell thickness is much larger. Nanocrystal parameters finally deduced from the simulation method are  $9.3 \pm 0.2$  Å and  $24 \pm 6$  Å for the CdSe shell and ligand layer thickness, respectively. The former value correlates very well with data of Cao and Banin<sup>4</sup> and is equivalent to  $2.1 \pm 0.1$  monolayers of zincblende CdSe in the (110) orientation. The value for the organic layer, i.e., the average thickness over many nanocrystals, is however quite large. Previously this method yielded a result of 12.3 Å for the TOP layer on a InP/ZnS core-shell system<sup>20</sup> which agrees well with the expected length of 10 to 11 Å. Our value here is quite high and implies that more than a single monolayer of TOP molecules surround the InAs/CdSe system. It is important to note that this might simply be a result of the sample preparation for the x-ray photoelectron spectroscopy (XPS) measurements. When the nanocrystals are deposited on the Au foil and the solvent evaporates, some free TOP molecules present in the solution might additionally condense on the nanocrystal film and therefore lead to a larger TOP layer thickness. Coverage of the crystals in solution with more than one layer of TOP is unlikely. Since the simulation method is much more sensitive to the CdSe shell dimensions, we again emphasize that uncertainties relating to the ligand shell only negligibly effect our result for the CdSe shell thickness.

#### IV. SUMMARY

We have found the physical origin for the improved photoluminescence yield of InAs/CdSe core-shell nanocrystals as compared to that of the pure InAs system. In the latter, surface traps provide dark recombination channels for the Wannier excitons and removal of these traps is caused by forming chemical bonds between both In and As surface atoms with the epitaxial shell layer above. Surface states in the InAs nanocrystals are likely to be present on both anion and cation sites which implies that dark channel exciton recombination relies on charge traps for both electrons and holes. Highly photoluminescent nanocrystals have useful applications in biological labeling experiments and are also essential for nanoscale optoelectronic devices. Our results should be useful toward a full description of how the luminescence yield is optimized as well as describing the relationship between electronic and crystal structure at a nanocrystal surface.

\*Corresponding author.

Electronic address: mcginley@mail.desy.de

- <sup>1</sup>H. Weller, *Angew. Chem., Int. Ed. Engl.* **32**, 41 (1993).
- <sup>2</sup>A. Mews, A. Eychmüller, M. Grieg, D. Schoos, and H. Weller, *J. Phys. Chem.* **98**, 934 (1994).
- <sup>3</sup>O. Millo, D. Katz, Y.-W. Cao, and U. Banin, *Phys. Rev. Lett.* **86**, 5751 (2001).
- <sup>4</sup>Y.-W. Cao and U. Banin, *J. Am. Chem. Soc.* **122**, 9692 (2000).
- <sup>5</sup>X. Peng, M.C. Schlamp, A.V. Kadavanich, and A.P. Alivisatos, *J. Am. Chem. Soc.* **119**, 7019 (1997).
- <sup>6</sup>M.A. Hines and P. Guyot-Sionnest, *J. Phys. Chem.* **100**, 462 (1996).
- <sup>7</sup>H. Yang and P.H. Holloway, *Appl. Phys. Lett.* **82**, 1965 (2003).
- <sup>8</sup>A.A. Guzelian, U. Banin, A.V. Kadavanich, X. Peng, and A.P. Alivisatos, *Appl. Phys. Lett.* **69**, 1432 (1996).
- <sup>9</sup>N. Tessler, V. Medvedev, M. Kazes, S.H. Kann, and U. Banin, *Science* **295**, 1506 (2002).
- <sup>10</sup>M.P. Bruchez, M. Moronne, P. Gin, S. Weiss, and A.P. Alivisatos, *Science* **281**, 2013 (1998).
- <sup>11</sup>J. Nanda and D.D. Sarma, *J. Appl. Phys.* **90**, 2504 (2001).
- <sup>12</sup>J.N. Andersen and U.O. Karlsson, *Phys. Rev. B* **41**, 3844 (1990).
- <sup>13</sup>C.B.M. Andersson, U.O. Karlsson, M.C. Håkansson, L.Ö. Olsson, L. Ilver, J. Kanski, and P.-O. Nilsson, *Surf. Sci.* **347**, 199 (1996).
- <sup>14</sup>G. LeLay, D. Mao, A. Kahn, Y. Hwu, and G. Margaritondo, *Phys. Rev. B* **43**, 14301 (1991).
- <sup>15</sup>J.M.C. Thornton, P. Weightman, D.A. Woolf, and C.J. Duncombe, *Phys. Rev. B* **51**, 14459 (1995).
- <sup>16</sup>C. McGinley, M. Riedler, T. Möller, H. Borchert, S. Haubold, M. Haase, and H. Weller, *Phys. Rev. B* **65**, 245308 (2002).
- <sup>17</sup>G. Bratina, T. Ozzello, and A. Franciosi, *J. Vac. Sci. Technol. A* **14**, 3135 (1996).
- <sup>18</sup>T. Scimeca, Y. Watanabe, R. Berrigan, and M. Oshima, *Phys. Rev. B* **46**, 10201 (1992).
- <sup>19</sup>H. Fu and A. Zunger, *Phys. Rev. B* **56**, 1496 (1997).
- <sup>20</sup>H. Borchert, S. Haubold, M. Haase, H. Weller, C. McGinley, M. Riedler, and T. Möller, *Nano. Lett.* **2**, 151 (2002).
- <sup>21</sup>C. McGinley, H. Borchert, M. Pflughoefft, S. Al Moussalami, A.R.B. de Castro, M. Haase, H. Weller, and T. Möller, *Phys. Rev. B* **64**, 245312 (2001).
- <sup>22</sup>D.R. Penn, *Phys. Rev. B* **35**, 482 (1987).
- <sup>23</sup>S. Tanuma, C.J. Powell, and D.R. Penn, *Surf. Interface Anal.* **21**, 165 (1993).